Since January 2020 Elsevier has created a COVID-19 resource centre with free information in English and Mandarin on the novel coronavirus COVID-19. The COVID-19 resource centre is hosted on Elsevier Connect, the company's public news and information website.

Elsevier hereby grants permission to make all its COVID-19-related research that is available on the COVID-19 resource centre - including this research content - immediately available in PubMed Central and other publicly funded repositories, such as the WHO COVID database with rights for unrestricted research re-use and analyses in any form or by any means with acknowledgement of the original source. These permissions are granted for free by Elsevier for as long as the COVID-19 resource centre remains active.

Computers in Biology and Medicine 134 (2021) 104464

Contents lists available at ScienceDirect

Computers in Biology and Medicine

journal homepage: www.elsevier.com/locate/compbiomed

The interaction of the bioflavonoids with five SARS-CoV-2 proteins targets: An *in silico* study

Ganesh Prasad Mishra [a,**,1], Rajendra N. Bhadane [b,c,1], Debadash Panigrahi [d], Haneen A. Amawi [e], Charles R. Asbhy Jr. [f], Amit K. Tiwari [g,h,*]

[a] Kharvel Subharti College of Pharmacy, Swami VivekanandSubharti University, Subhartipuram, NH-58, Delhi-Haridwar Bypass Road, Meerut, U.P, 250005, India
[b] Structural Bioinformatics Laboratory, Faculty of Science and Engineering, Biochemistry, Åbo Akademi University, FI, 20520, Turku, Finland
[c] Pharmaceutical Sciences Laboratory, Faculty of Science and Engineering, Pharmacy, Åbo Akademi University, FI, 20520, Turku, Finland
[d] Drug Research Laboratory, Nodal Research Centre, College of Pharmaceutical Sciences, Puri, Baliguali, Puri- Konark Marine Drive Road, Puri, Odisha, 752002, India
[e] Department of Clinical Pharmacy and Pharmacy Practice, College of Pharmacy, Yarmouk University, Shafiq Irshidat St, Irbid, Jordan
[f] Department of Pharmaceutical Sciences, College of Pharmacy & Pharmaceutical Sciences, St. John's University, Queens, NY, USA, 10049
[g] Department of Pharmacology & Experimental Therapeutics, College of Pharmacy & Pharmaceutical Sciences, The University of Toledo, Toledo, OH, 43614, USA
[h] Department of Cancer Biology, College of Medicine & Life Sciences, The University of Toledo, Toledo, OH, 43614, USA

ARTICLE INFO

Keywords:
Docking
Molecular dynamics (MD)
Binding free energy
MMGBSA
SARS-CoV-2
Flavonoids

ABSTRACT

Flavonoids have been shown to have antioxidant, anti-inflammatory, anti-proliferative, antibacterial and anti-viral efficacy. Therefore, in this study, we choose 85 flavonoid compounds and screened them to determine their *in-silico* interaction with protein targets crucial for SARS-CoV-2 infection. The five important targets chosen were the main protease (Mpro), Spike receptor binding domain (Spike-RBD), RNA - dependent RNA polymerase (RdRp or Nsp12), non-structural protein 15 (Nsp15) of SARS-CoV-2 and the host angiotensin converting enzyme-2 (ACE-2) spike-RBD binding domain. The compounds were initially docked at the selected sites and further evaluated for binding free energy, using the molecular mechanics/generalized Born surface area (MMGBSA) method. The three compounds with the best binding scores were subjected to molecular dynamics (MD) simulations. The compound, tribuloside, had a high average binding free energy of −86.99 and −88.98 kcal/mol for Mpro and Nsp12, respectively. The compound, legalon, had an average binding free energy of −59.02 kcal/mol at the ACE2 spike-RBD binding site. The compound, isosilybin, had an average free binding energy of −63.06 kcal/mol for the Spike-RBD protein. Overall, our results suggest that tribuloside, legalon and isosilybin should be evaluated in future studies to determine their efficacy to inhibit SARS-CoV-2 infectivity.

1. Introduction

Currently, numerous research groups are developing compounds and vaccines for the treatment of patients infected with SARS-CoV-2 [1]. Several strategies have been used to develop drugs to treat SARS-CoV-2. Unfortunately, due to restrictions regarding the use of SARS-CoV-2 (i.e. biosafety level III requirements) and an ongoing pandemic, laboratory research has been greatly limited. Computational tools have been widely used for development of variety of drugs including this study by screening libraries to discover compound that could affect the attachment, maturation and replication of SARS-CoV-2 [2,3]. The major focus of these studies was to obtain information about the SARS-CoV-2 proteins and target them with natural phytochemicals. The major targets studied were the SARS-CoV-2 main protease (Mpro) [4], spike glycoprotein-receptor binding domain (Spike-RBD) [5], angiotensin-converting enzyme-2 (ACE2) [6], RNA-dependent RNA polymerase (RdRp; also known as non-structural protein 12(Nsp12)) [7] and non-structural protein 15 (Nsp15) [8]. The protein, Mpro, also known as the 3C-like protease, is required for the proteolytic maturation of the SARS-CoV-2 [9]. It is also essential for the regulation and cleavage of the polyproteins, pp1a and pp1ab, that generates functional proteins, such as Nsp12, Nsp15 and exoribonuclease [10,11]. The inhibition of this enzyme prevents viral maturation and increases the host immune

* Corresponding author. Department of Pharmacology & Experimental Therapeutics, College of Pharmacy & Pharmaceutical Sciences, The University of Toledo, Toledo, OH, 43614, USA.
** Corresponding author.
E-mail addresses: gm25mishra@gmail.com (G.P. Mishra), amit.tiwari@utoledo.edu (A.K. Tiwari).
[1] The first two authors contributed equally to the manuscript.

https://doi.org/10.1016/j.compbiomed.2021.104464
Received 21 January 2021; Received in revised form 23 April 2021; Accepted 28 April 2021
Available online 10 May 2021
0010-4825/© 2021 Published by Elsevier Ltd.

List of abbreviations

Mpro, Main protease;
SGp-RBD, Spike glycoprotein-receptor binding domain;
ACE2, Angiotensin-converting enzyme-2;
RdRp, RNA dependent RNA polymerase;
non-structural protein 12, Nsp12;
non-structural protein 15 or Endoribonuclease, Nsp15;
SARS-CoV-2, Severe acute respiratory syndrome coronavirus 2;
COVID-2, Coronavirus disease;
Molecular Mechanics/Generalized Born Surface Area, MM-GBSA;
root-mean-square deviation, RMSD

response to SARS-CoV-2 [12,13]. The spike protein, or S protein of SARS-CoV-2, mediates viral infection and is involved in viral pathogenesis [14]. The S1 subunit of the S protein recognizes and binds to the host receptor, angiotensin-converting enzyme 2 (ACE2), which induces the cleavage of the spike protein that produces a conformational change in S2 region to facilitate the fusion of the viral envelope with the host cell membrane [1,15]. The region of the S protein that binds to ACE2 receptor is the receptor-binding domain (RBD) or Spike-RBD [16]. The ACE2 receptor is a transmembrane metalloproteinase that is a functional receptor for SARS-CoV-2 [17,18]. The interaction between the viral S protein and ACE2 trimerizes the S glycoprotein, producing the internalization of the virus by the host cell [19]. Therefore, the ACE2 and S proteins are important drug targets for preventing the entry of SARS-CoV-2 into the host cell [20]. The non-structural protein 12, in combination with the non-structural proteins 7 and 8, catalyzes the synthesis of a positive-stranded RNA molecule that is required for viral translation and replication and thus, infectivity [21,22]. A number of studies have reported that the inhibition of the Nsp12 by compounds such as favipiravir and remdesivir, inhibits the *in vitro* and *in vivo* replication of SARS-CoV-2, thereby significantly decreasing infectivity [23,24]. Finally, the coronavirus uridylate-specific endoribonuclease, Nsp15, a highly conserved protein among vertebrate nidoviruses, has been suggested to be a target for the development of drugs for SARS-CoV-2 [25]. Nsp15 mediates replication and the processing of sub-genomic RNAs during the replication cycle and it biodegrades viral polyuridine sequences to decrease the detection of the virus by the immune system of the host cell [26].

It has been reported that natural phytochemicals, such as certain bioflavonoids, have efficacy against viruses such as the dengue virus, herpes simplex virus (HSV), Japanese encephalitis virus and Ebola [27–32]. In addition, certain bioflavonoid compounds have *in vitro* and *in vivo* anti-inflammatory and anti-oxidant efficacy [33]. Thus, it is possible that bioflavonoids could have efficacy in the treatment of SARS-CoV-2 by decreasing viral infectivity and replication and/or decreasing the inflammatory response. The identification of naturally-derived *anti*-SARS-CoV-2 compounds can be done by screening various databases/libraries using computational approaches, such as molecular docking, pharmacophore mapping, 3D-QSAR and molecular dynamics (MD) simulations [34–41]. The computational screening approach is advantageous at this time due to the limited access to laboratories and researchers can focus on the outcome of these studies, which could represent a platform for the design and development of novel compounds within a relatively short period of time [42].

In this study, we screened 85 flavonoids that were previously reported to have antimicrobial and antioxidant efficacy based on docking scores and molecular mechanics/generalized Born surface area (MMGBSA) [43]. The purpose of the high-throughput screening was to identify compounds that have high docking scores for the active site of the SARS-CoV-2 proteins, Mpro, SpikeRBD, Nsp12 and NSP15 in SARS-CoV-2 and the host ACE-2 receptor.

2. Material and methods

2.1. Platform for molecular modeling

All computational studies and visualization of the protein-ligand complexes were performed using the Schrodinger drug discovery suite (Release 2020-4: Schrödinger, LLC, New York, NY, 2020) and Pymol version 2.4.1 [44].

2.2. Flavonoid compounds library preparation

A dataset of 85 flavonoid molecules, with known antiviral and antimicrobial efficacy, were selected from the PubChem database (www.pubchem.ncbi.nlm.nih.gov) and their *in silico* interaction with the SARS-CoV-2 target proteins was determined for binding energy [Suppl file Table 1]. The SDF files of the compounds were imported to the Maestro molecular modeling suite. The LigPrep tool of Maestro (Schrödinger Release 2020-4) was used to generate optimized, low-energy conformers of the ligands using the OPLS3e force field [45]. Possible tautomeric states were generated for each ligand at a pH of 7.0 ± 2.0 using the Epik [46,47]. The specified chirality was retained and a maximum of 32 stereoisomers were generated per ligand. This approach yielded 843 structures generated from the 85 selected compounds and were used for docking and to estimate binding free energy.

2.3. Protein preparation

Based on the available 3D structures of the target proteins, high resolution structures were retrieved from the protein data bank (PDB) [48]. The structures of the SARS-CoV-2 main protease (Mpro) (PDB ID: 6LU7) [49], the non-structural protein 12 (nsp12) (PDB ID: 7BV2) [42] and non-structural protein 15 (nsp15) (PDB ID: 6WXC) [43], were complexed with a co-crystallized inhibitor. The structure of the spike receptor binding domain was complexed with the angiotensin-converting enzyme-2 (ACE2) without a co-crystallized inhibitor (PDB ID: 6M0J) [44]. Using the Protein Preparation Wizard of Maestro, the selected structures were processed as as per the general protocol. Briefly, the missing hydrogen atoms were added to the structure and the hydrogen bond network was optimized using PROPKA at pH 7.0. All water molecules beyond 3 Å were removed and a restrained minimization was conducted using the OPLS3e force field with a convergence criterion of 0.3 Å root-mean-square deviation (RMSD) for all the heavy atoms. The histidine protonation state for the structures of Mpro and Nsp15 were given specific attention. The histidine protonation network for SARS-CoV-2 Mpro was optimized as per our previous protocol [50]. While processing the structure of Nsp15, the protonation state was optimized using an interactive H-bond optimiser panel usinf PROPKA at pH 7.0. The His-250 residue was kept delta protonated (HID-250), whereas His-235 was eta protonated (HIE-235) as previously reported [11].

2.4. Docking protocol

For docking with the SARS-CoV-2 main protease, Nsp12 and Nsp15, the coordinates of the co-crystallized ligands were used to prepare the receptor grid. For the spike RBD and ACE2, the binding site was defined based on the interactions between the interfaces of spike and ACE2 protein. The receptor grid generation tool of the docking program Glide in Maestro was used to define the docking site for the target proteins [51–53]. The partial charge limit was 0.25 and the van der Waals scaling factor was 0.80. While preparing the grid for the target proteins, the size of the outer box of the docking grid was fixed at 30 Å × 30 Å × 30 Å and the inner box dimensions were 10 Å × 10 Å × 10 Å. The size of the ligands to be docked was ≤20 Å. The docking was conducted using the

Table 1
Docking score and binding free energy values for the SARS-CoV-2 Mpro active site.

Ligand	Docking score	Binding free energy by MMGBSA (ΔG_{bind} in kcal/mol)	Average binding free energy by MMGBSA from last 50ns MD simulation (ΔG_{bind} in kcal/mol)
N3 peptide	-9.55	-79.8[#]	-98.97[#]
Tribuloside	-8.767	-93.55	-86.99
Panasenoside	-9.958	-84.33	-73.90
Monoxerutin	-13.612	-78.88	-76.10
Hirsutrin	-10.318	-74.77	
Legalon	-7.591	-74.65	
Tiliroside	-8.445	-74.14	
Kaempferitrin	-9.279	-73.45	
Oenin	-3.871	-72.16	
Isorhoifolin	-8.673	-71.86	
Neosakuranin	-9.397	-71.43	

Note: The color scheme of green-white-red indicates the affinity values from the highest, medium and lowest, respectively, for the protein target. [#]The binding affinity was calculated for the non-covalently bound pose.

Glide extra precision (XP) modes with flexible ligand sampling. The Epik state penalties were added to the final docking scores. For each ligand, ten poses were used for post-docking minimization. A maximum one pose per ligand was generated. The docking protocol for Mpro, Nsp12 and Nsp15 was validated by redocking the co-crystallized ligand with their respective crystal positions.

2.5. Binding free energy estimation

The output pose viewer file from the Glide XP docking was used as an input to re-rank the compounds using the Prime MM-GBSA binding energy [54,55] values calculated with implicit solvation model (VSGB2.1) in the OPLS3e force field. The binding free energy ΔG_{bind} was calculated using the following equation:

$$\Delta G_{bind} = \Delta E_{MM} + \Delta G_{solv} + \Delta G_{SA}$$

where ΔE_{MM} is the difference in energy between the complex structure and the sum of the energies of the ligand and unliganded receptor. The ΔG_{solv} is the difference in the GBSA solvation energy of the complex and the sum of the solvation energies for the ligand and unliganded receptor. The ΔG_{SA} is the difference in the surface area energy for the complex and the sum of the surface area energies for the ligand and uncomplexed receptor. The Prime/MM-GBSA energies after MD simulation were calculated from the last 50 ns of the simulation trajectories.

2.6. Molecular dynamics (MD) simulation

The highest scoring ligand-protein complexes, with high binding free energies (ΔG_{Bind}) and/or Glide docking scores, were submitted to a 100ns molecular dynamics (MD) simulation using Desmond (Schrödinger Release 2020-4: Desmond Molecular Dynamics System, D. E. Shaw Research, New York, NY, USA, 2020) [56]. The simulation was used to refine the docked poses and evaluate the stability of binding at the active sites on the target proteins. In order to compare the efficiency of these screened compounds, the native crystal complexes of Mpro, Nsp12 and Nsp15 were simulated using the same protocol. The simulation systems were prepared using the System Builder tool of the Desmond module. The single point charge (SPC) water [57] was chosen as the explicit solvation model. Each system was neutralized using an appropriate number of Na+ or Cl-counter ions. An orthorhombic simulation box, with Periodic Boundary Conditions (PBC) and a 10 Å buffer space between the solute and the box edge, was used for each system. The simulation systems were minimized and equilibrated before the actual simulations and before production simulation in a stepwise manner. After system relaxation, the production simulation was performed using the NPT ensemble for 100 ns, using a reversible reference system propagator algorithms (RESPA) integrator [56]. The temperature (300 K) was set using the Nosé–Hoover chain thermostat [58–60], with a relaxation time of 1.0 ps. The pressure was set at 1.01325 bar with the Martyna–Tobias–Klein barostat [61], using isotropic coupling and a relaxation time of 2.0 ps. Long-range interactions were handled using the U-series method [62] and for short range interactions, a cut-off radius of 9.0 Å was used. The MD trajectories were analyzed using the Maestro built-in Simulation Interactions Diagram tool and Microsoft Excel360.

2.7. Docking validation

The docked poses of co-crystallized complexes were redocked at their respective binding sites to determine the precision of the docking protocol we used for Mpro, Nsp12 and Nsp15.

3. Results

3.1. Computational screening of the therapeutic targets of SARS-CoV-2

The ligprep generated 843 structures of the flavonoid's compounds from the original 85 entries that were subjected to brief molecular docking and a binding free energy estimation protocol. The compounds were then selected based on binding free energy, docking scores and individual observation of each pose at the binding sites. For each target, the 10 compounds with best docking pose were identified. The molecular dynamics (MD) simulation of the best 3 compounds at each of the targets were selected and subjected to 100 ns MD simulation. The RMSD and RMSF graphs for Cα carbon atoms were plotted. The interaction of the ligand with each protein was performed. The average binding free energy calculated by Prime-MM/GBSA method was based on the last 50 ns MD simulation.

3.1.1. SARS-CoV-1 main protease (Mpro) site

The docking and subsequent binding free energy estimation yielded the top 10 flavonoids (Table 1). The monoxerutin shows the highest docking score among all the compounds at the Mpro site. The MMGBSA-based binding free energy for monoxerutin was −78.88 kcal/mol, which is comparable to that of peptide inhibitor, N3. Furthermore, the compounds, tribuloside and panasenoside, had a greater interaction with mPro compared to co-crystallized N3. All of the top 10 compounds had a binding free energy > −70 kcal/mol (Table 1).

3.1.2. The spike -receptor binding domain (Spike-RBD) site

The glycosylated spike protein (S-protein) directly interacts with the human angiotensin-converting enzyme 2 (ACE2) receptor via the receptor-binding domain (RBD) of the S-protein [63]. As the S-protein is exposed to the surface and is essential for viral entry into the host cells, the S-protein is considered to be a first-line therapeutic target for the treatment of SARS-CoV-2 infection [64]. The MMGBSA - based binding free energy for isosilybin was −68.39 kcal/mol and this value was the highest compared to the other flavonoids for the Spike RBD. Table 2 shows the 10 compounds with the highest scores for the RBD of spike, with binding free energy > −50 kcal/mol before MD simulation.

3.1.3. Angiotensin converting enyme-2(ACE-2) spike protein binding site

The angiotensin-converting enzyme-2 (ACE-2) is a receptor that binds the spike protein of SARS-CoV-2, which activates the host cell protease and produces the fusion of the spike protein with host cell membrane [1]. Consequently, the inhibition of the binding of the spike protein with the ACE-2 protein could be an effective strategy to prevent SARS-CoV-2 infeciton [1]. The flavonoids with the highest docking scores are shown in Table 3. For the ACE-2 spike protein binding site, isorhoifolin had the highest docking score, whereas kikviritin had the lowest docking score. The MMGBSA based binding free energy for legalon was −54.6 kcal/mol.

3.1.4. The non-structural protein-12 (Nsp12)

The RNA-dependent RNA polymerase (RdRp), also known as Nsp12, catalyzes the synthesis of viral RNA, in combination with cofactors Nsp-7 and Nsp-8, within the host cell and plays a major role in the replication and transcription of SARS-CoV-2 [65]. In this study, we docked the compounds at Nsp12 using co-ordinates for co-crystallized remdesivir (Table 4). The flavonoids, isoorientin and tribuloside, had significantly greater docking scores of −10.96 and −11.571 kcal/mol, respectively, compared to −6.244 kcal/mol for remdesivir (it is important to note that it can form a covalent bond at this site). Similarly, the binding free energy of isoorientin and tribuloside for Nsp12 were appreciable compared to remdesivir.

3.1.5. Molecular docking with endoribonuclease (NSP15)

The non-structure protein, Nsp15, is essential in the life cycle and virulence of SARS-CoV-2 [66]. We performed docking and MMGBSA analysis of our compounds at the tipiracil binding site and the results are presented in Table 5. The 10 compounds with the highest docking scores compounds at the tipiracil binding site were > - 4 kcal/mol, except for tribuloside. The docking scores and binding free energy value of Persiconin and Neosakuranin were comparable to that of Tipiracil co-crystallized at the tipiracil binding site on Nsp15.

3.1.6. Validation of docking

Before performing the docking analysis at these selected sites, the redocking of co-crystallized inhibitors was performed where the structure of the co-crystallized inhibitor was available. Unfortunately, we could not validate the docking performed at the ACE2 and Spike RBD site due to unavailability of the co-crystalized inhibitor complex at the interface between ACE2 and the Spike RBD. At the N3 and remdesivir binding sites, redocking was performed by cleaving the covalent bond using the 3D builder tool of maestro, which does not change the actual orientation of the groups after regenerating the original structure of ligand and amino acid side chain. Our results indicated a slight deviation in the orientation of N3 during redocking that was due to the larger size of this peptide ligand as we were able to generate very accurate redocked poses at the other two sites (Fig. 1).

4. Discussion

Numerous studies have reported that flavonoids and their derivatives are efficacious *in vitro* in several viral strains, including avian influenza strain H5N1, HIV, HSV and Ebola [67]. In this study, we used an *in silico* approach to screen a library of 85 flavonoids to identify compounds that have a high binding affinity for the critical SARS-CoV-2 proteins, main protease (Mpro), receptor binding domain of spike protein- (Spike-RBD), angiotensin-converting enzyme-2 (ACE-2), non-structural protein 12 and non-structural protein 15.

The active site of SARS-CoV-2 Mpro has been reported to have 4 subsites: S1′, S1, S2 and S4 [49]. The catalytic Cys-145 and His-163 are located in the S1' site. The Glu-166 residue is in the S1 pocket, whereas Met-165 and Val-186 are in the S2 pocket and Pro-168 and Gln-189 are located in the S4 site [49]. As compared to other receptor sites in the SARS-Cov-2 proteins, the Mpro site is comparatively flexible and can accommodate a wide variety of ligands, including peptides and small molecules [68]. This characteristic is important as it makes the docking critical because many compounds could have appreciable docking scores at this site. Consequently, the use of MD simulation is critical for determining stable interactions between the screened compounds and the docking site. As shown in Fig. 2, certain flavonoid compounds formed an efficient hydrogen bond network with key amino acids and the details of these interactions are shown in the supplementary results [see suppl file- Figure S1, S6, S11, S16].

Tribuloside had the highest magnitude of interaction among all of the compounds for Mpro, based on the binding free energy before and after MD simulation. There was a slight decrease in initial interaction energy from −93.55 to −86.99 kcal/mol during the simulation. However, it is important to note that the latter value is the average binding score, which suggests that it could inhibit Mpro if tested *in vitro,*

Table 2
Docking score and binding free energy values for the SARS-CoV-2 Spike RBD active site.

Ligand	Docking score	Binding free energy by MMGBSA (ΔG_{bind} in kcal/mol)	Average binding free energy by MMGBSA from last 50ns MD simulation (ΔG_{bind} in kcal/mol)
Isosilybin	-5.191	-68.39	-63.06
Panasenoside	-6.919	-66.9	-55.81
Rhoifolin	-6.911	-64.62	-
Helichrysoside	-5.684	-63.86	-49.62
Tribuloside	-5.723	-62.85	-
Biorobin	-6.407	-60.84	-
Legalon	-4.649	-60.70	-
Troxerutin	-7.031	-60.65	-
Oenin	-4.497	-59.44	-
Kuromanin	-3.366	-57.83	-

Note: The color scheme of green-white-red indicates the affinity from the highest, medium and lowest, respectively, for the protein target.

Table 3
Docking score and binding free energy values for the SARS-CoV-2 SpikeRBD active site of the human ACE2 receptor.

Ligand	Docking score	Binding free energy by MMGBSA (ΔG_{bind} in kcal/mol)	Average binding free energy by MMGBSA from last 50ns MD simulation (ΔG_{bind} in kcal/mol)
Legalon	-2.785	-54.6	-59.02
Isorhoifolin	-6.387	-48.40	-31.28
Genistoside	-4.962	-48.17	-41.20
Isosilybin	-4.479	-47.73	-
Sissotrin	-4.849	-47.27	-
Tribuloside	-3.939	-47.18	-
Persiconin	-3.888	-46.36	-
Likviritin	-2.51	-46.24	-
Helichrysoside	-8.074	-45.96	-
Genistoside	-5.734	-45.71	-

Note: The color scheme of green-white-red indicates the affinity from the highest, medium and lowest, respectively.

Table 4
Docking score and binding free energy values for t remdesivir at the SARS-CoV-2 protein, Nsp12.

Ligand	Docking score	Binding free energy by MMGBSA (ΔG_{bind} in kcal/mol)	Average binding free energy by MMGBSA from last 50ns MD simulation (ΔG_{bind} in kcal/mol)
Remdesivir	-6.244	-39.44[#]	-43.34[#]
Isoorientin	-10.96	-70.1	-86.29
Tribuloside	-11.571	-64.62	-88.98
Silybin	-9.948	-55.09	-80.56
Legalon	-8.442	-50.45	-
Isosilybin	-8.93	-50.31	-
Puddumin A	-9.285	-46.49	-
Hirsutrin	-10.564	-42.99	-
Hirsutrin	-10.095	-41.31	-
Guaijaverin	-9.781	-40.16	-
Magnoflorine	-5.998	-38.73	-

Note: The color scheme of green-white-red indicates the affinity from the highest, medium and lowest values, respectively. [#]The binding affinity calculated for non-covalently bound pose

Table 5
Docking scorse and binding free energy values at the tipiracil binding site on SARS-CoV-2 Nsp15.

Ligand	Docking score	Binding free energy by MMGBSA (ΔG_{bind} in kcal/mol)	Average binding free energy by MMGBSA from last 50ns MD simulation (ΔG_{bind} in kcal/mol)
Tipiracil_co-crystallised	-5.58	-46.87	-34.02
Persiconin	-4.164	-50.62	-26.60
Isorhoifolin	-3.841	-48.77	-25.50
Neosakuranin	-6.634	-48.53	-
Biorobin	-5.502	-48.36	-22.67
Genistoside	-5.548	-47.8	-
Tribuloside	-0.289	-47.52	-
Rhoifolin	-6.037	-47.12	-
Silybin	-4.555	-44.96	-
Legalon	-5.221	-44.19	-
Puddumin A	-4.719	-44.1	-

Note: The color scheme of green-white-red indicates the affinity from the highest, medium and lowest values, respectively.

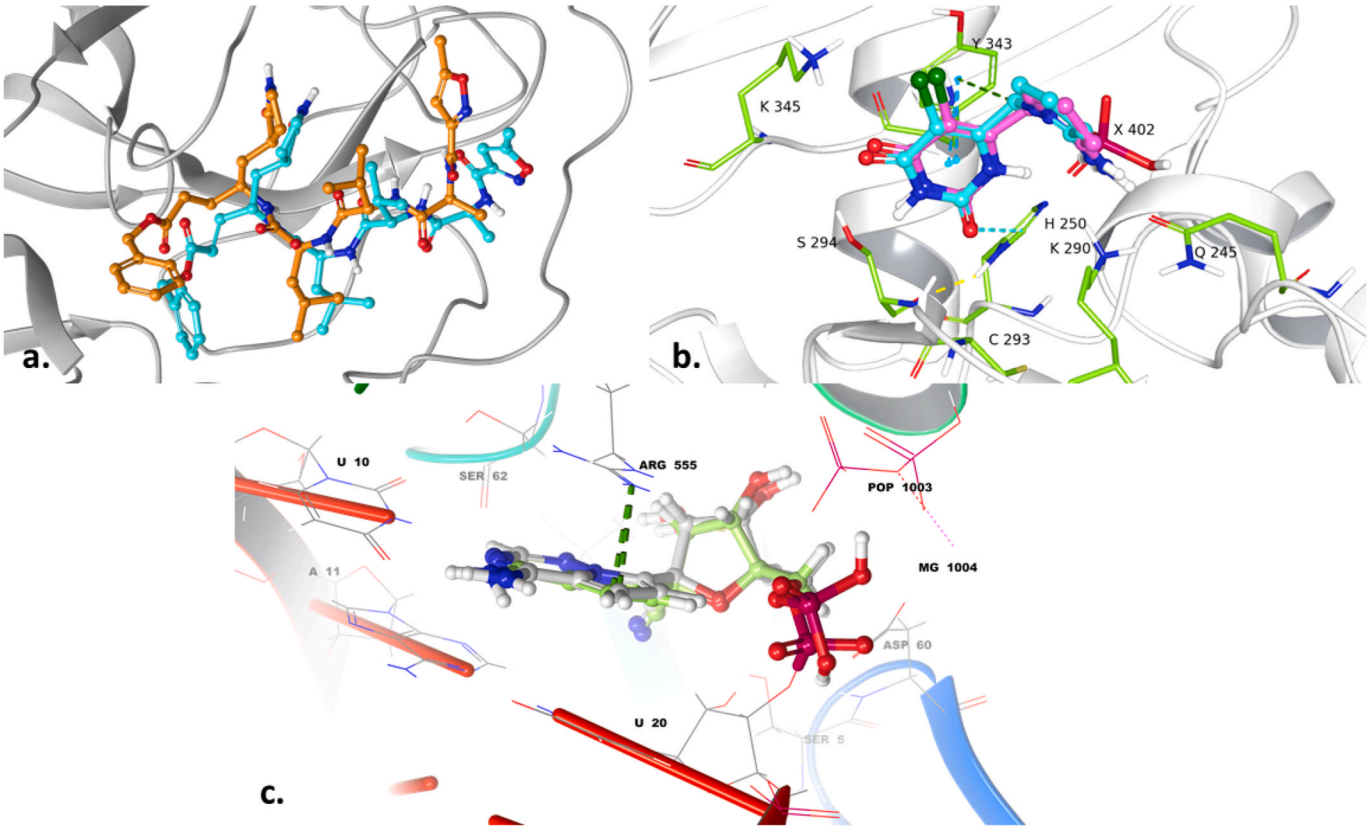

Fig. 1. a The redocked N3 peptide (cyancolour ball and stick representation), in grey, at the active site of SARS-CoV-2 Mpro (PDB ID: 6LU7) with co-crystallized. covalently bonded N3 peptide (represented by and orange ball and stick). **b.** Co-crystallized tipiracil (represented by a cyan colour ball and stick) and redocked tipiracil (represented by a pink ball and stick) showing key interactions (green sticks representing amino acids, phosphate groups represented as red sticks and interactions represented by cyan dash lines) with Nsp15 (grey cartoon representation). **c.** Co-crystallized and redocked remdesivir (represented by white and green balls and sticks, respectively) with Nsp12 protein (the interacting amino acids and RNA chains are represented by thin grey sticks). Nonpolar hydrogens are hidden for clarity.

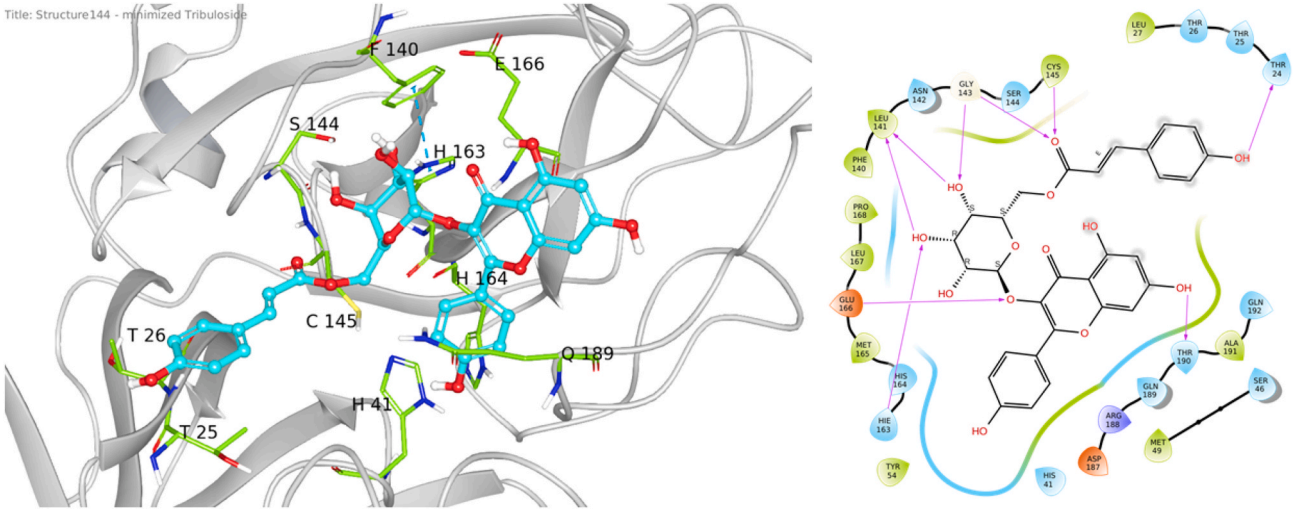

Fig. 2. The 3D structure of SARS-CoV-2 Mpro (PDB ID:6LU7) and its interaction with Tribuloside (left) and the ligand interaction in 2D (right side). The protein is represented in grey, tribuloside is represented by a cyan ball and sticks, amino acids are represented by green sticks (right) and donor and acceptor hydrogen bonds interactions are represented by pink arrows (left).

although this remains to be determined.

As with the ACE2 site, the binding pocket of RBD is also relatively shallow and the MD simulation for the ligand is important to determine the stability of the interactions of the compounds at this site. Furthermore, this will allow for the detection of false positive ligand poses during docking. Isosilybin had hydrogen bond interactions with Gly-202 and Gly-493, in addition to water mediated interactions with Thr-505, Arg-403 and Gly-498 (Fig. 3). Isosilybin also forms pi-pi interactions with Tyr-505, which increases the stability of its interaction with the binding pocket of RBD compared to panasenoside. Compared to

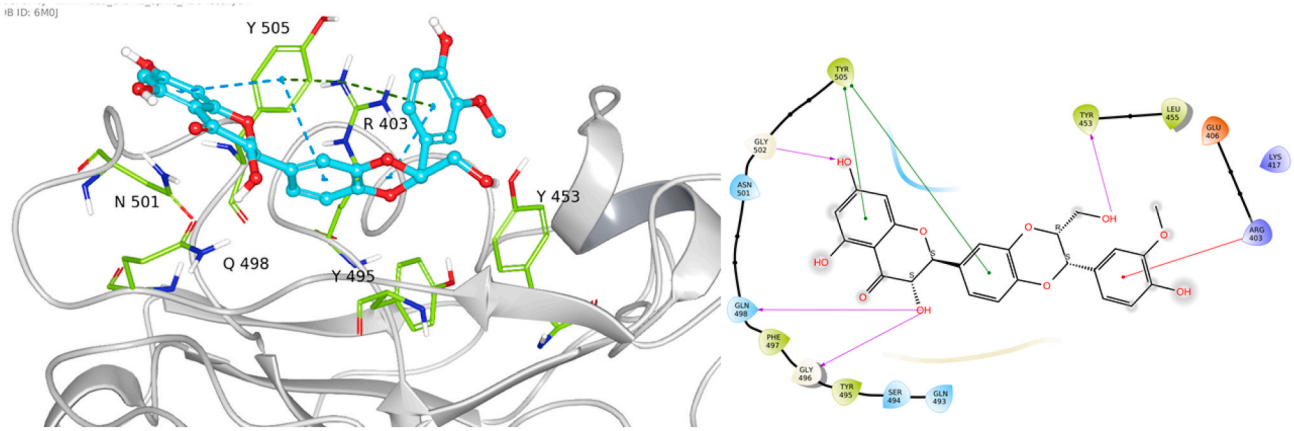

Fig. 3. The 3D structure of the interaction of SARS-CoV-2 Spike RBD protein (PDB ID:6MOJ) with isosilybin (left) and the ligand interaction in 2D(right side). The proteinis represented in grey, isosilybin represented by cyan balls and stick and the amino acids are represented by green sticks (right). The hydrogen bond interactions are represented in pink and the pi-pi interactions are represented by green arrows (left).

panasenoside and helichrysoside, whose interaction decreased after MD simulation, isosilybin had a better docking pose. [see suppl file-Figure S2, S7, S12, S17].

In this study, we selected a novel binding site when we conducted the docking poses at ACE2. The rationale behind the selection of this site was based on the fact that this site is in close proximity to the N-glycosylation site of ACE2, which occurs at the conserved residue, Asn-90 [69–72]. It has been reported that N-glycosylation of ACE2 and its inhibition by chloroquine and its derivatives could affect the binding of the Spike-RBD to the ACE2 receptor [51–54].

Fig. 4 shows the binding interactions of legalon at the ACE2 site. The major interactions between legalon and the ACE2 site involved Asn-90, Lys-26, Asp-30, His-34, Gly-37, Gly-96, Ala-387 and Arg-393. Additional details of the interactions are presented in the supplemental results (Figure S3, S8, S13, S18 in Suppl file). The interactions of legalon could affect SpikeRBD binding at this site and future *in vitro* studies should be done to verify this possibility.

The protein, Nsp12, in combination with the proteins, Nsp7 and Nsp8, is involved in the replication of the SARS-CoV-2 RNA genome [73]. Previous studies have reported that various flavonoids, including the compounds, C4, C8, C12, C16, C17, C20, C22, C23, calophyllolide, genistein, quercetin, tangeritin, arbutin and liquiritin, interact with the β-hairpin residues of Nsp12 [74]. The compounds we chose for MD simulation, tribuloside, isoorientin and silybin, had stable interactions at the remdesivir binding site is shown in Fig. 5. The rank order of the docking scores was tribuloside > isoorientin [see Suppl file-Figure S4, S9, S14, S19]. The root mean square fluctuation (RMSF) for the three compounds was convergent and was stable thought the MD simulation. The per residue interaction calculated using RMSF remained stable and was similar to the RMSF for the covalently bound, co-crystallized ligand, remdesivir.

Our results indicated that the active binding site of Nsp15 is highly specific for the uridine moiety of tipiracil and consequently, tipiracil inhibits Nsp15 and thus, it catalytic activity [57]. The uracil ring of tipiracil can stack against Tyr-341 and forms hydrogen bond interactions with Ser-294 and His-250. Our docking and binding free energy analysis indicated that certain flavonoid had high docking and binding free energy values at the active site of Nsp12. In addition, the compounds with the highest values were subjected to MD simulation but none of them maintained the initial interactions before simulation. The compounds, persiconin and isorhoifolin, had moderate interactions, whereas as biorobin lost significant interactions for Nsp12 after MD simulation. Furthermore, the RMSF did not converge well for biorobin. The detail binding interactions are shown in Fig. 6 and in the supplemental results [Suppl file-Figure S5, S10, S15, S20].

The coumarin ring of isorhoifolin and phenyl rings formed pi-pi interactions with Trp-333 and His-235 respectively. Isorhoifolin formed hydrogen bonds with Gly-285, Gly-151, Gly-189 and Thr-286. Similarly, periconin had significant interactions with Ser-316, Val-318, Trp-333, Leu-346 and Gly-347. However, none of the compounds formed the

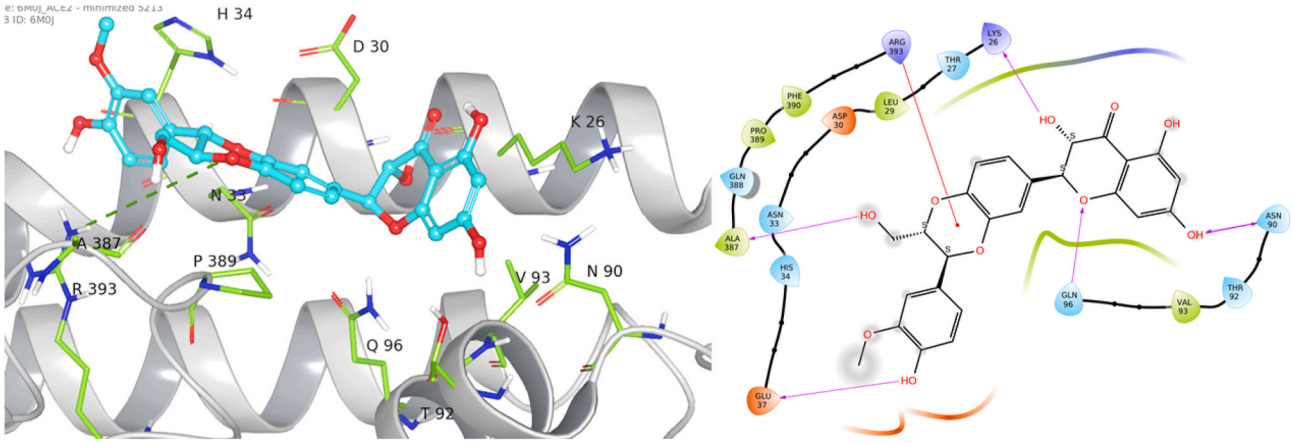

Fig. 4. The 3D structure of SpikeRBD binding domain of human ACE2 receptor (PDB ID:6MOJ) with Legalon (left) and ligand interaction in 2D view (right side). The protein is in grey cartoon representation, Legalon in cyan ball and sticks, amino acids in green sticks (right). The hydrogen bond interactions in pink and pi-pi interactions in green arrows (left).

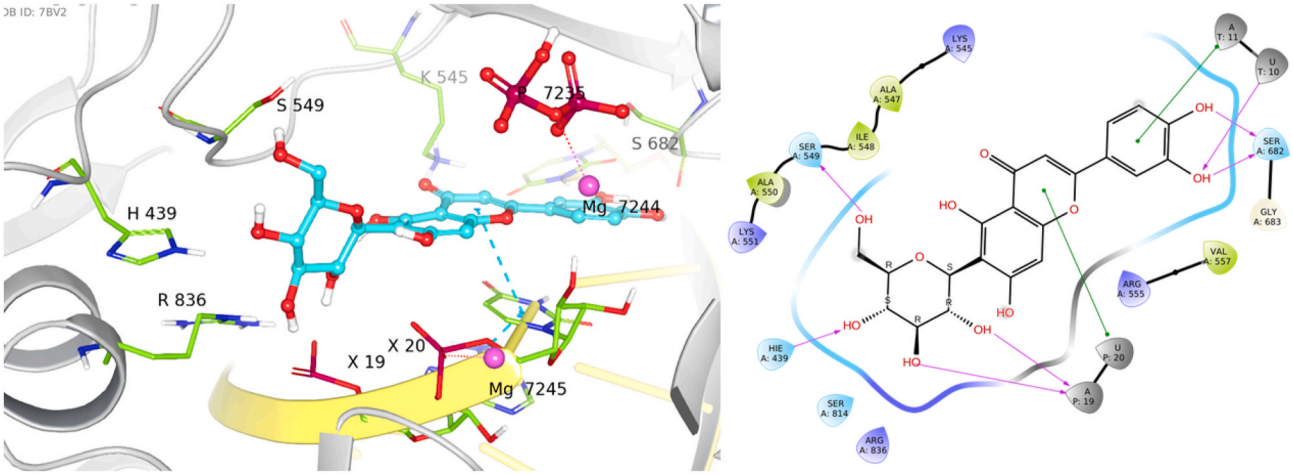

Fig. 5. The 3D structure of SARS-CoV-2 Nsp12 (PDB ID:7BV2), with Isoorientin (left) and the ligand interaction in 2D (right side). The protein is represented in grey, representation, isoorientin is represented by cyan balla and sticks, amino acids are represented by green sticks (right and the donor and acceptor hydrogen bond interactions are represented as pink arrows (left).

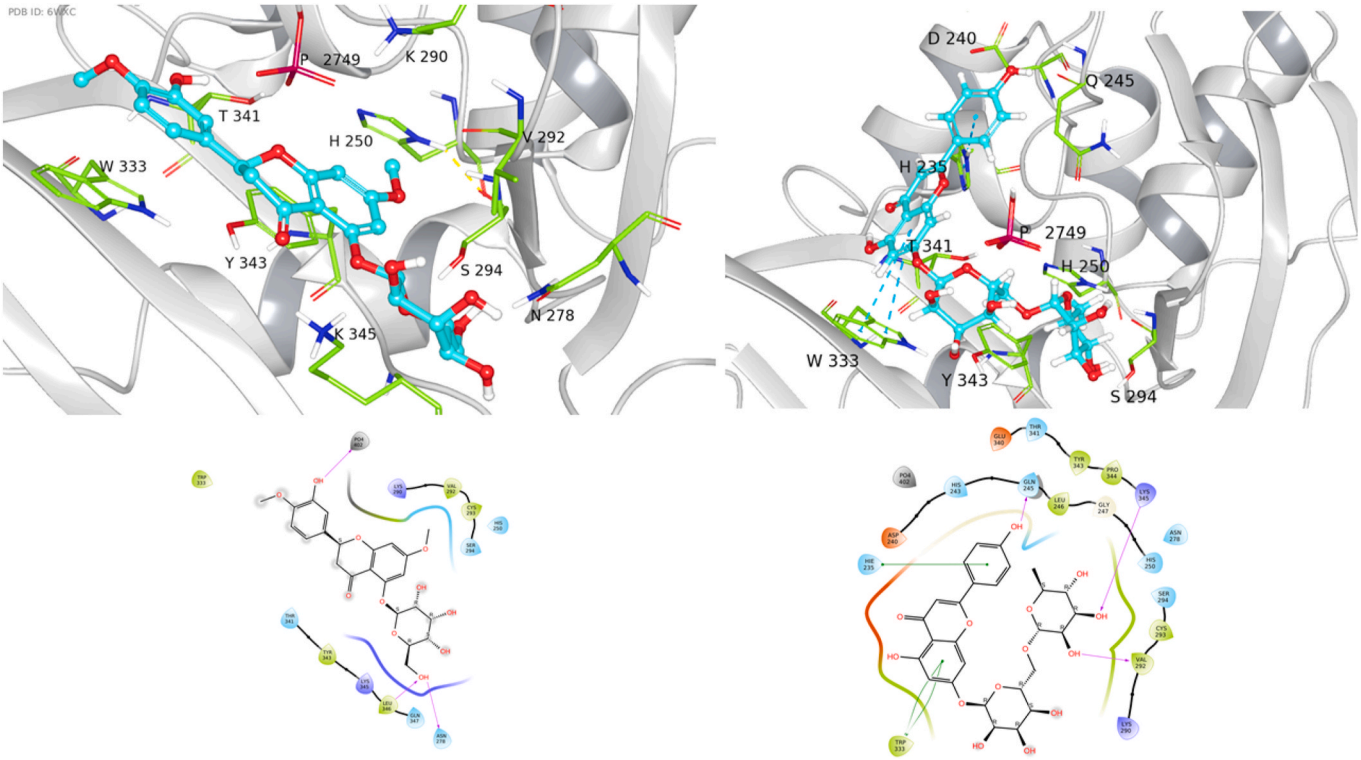

Fig. 6. The 3D structure of SARS-CoV-2 Nsp15 (PDB ID:6WXC) with Persiconin and (left) Isorhoifolin (right) and ligand interaction in 2D view (right side). The protein is in grey cartoon representation, Persiconin and Isorhoifolin in cyan ball and sticks, amino acids in green sticks (right), donor and acceptor hydrogen bond interactions in pink arrows (left), Non-polar hydrogens are hidden for clarity.

key interactions as observed for co-crystalized tipiracil. Also, none of the flavonoids interacted with key residues, such as Ser-294 and His-250.

5. Conclusion

In the present *in silico* study, 85 flavonoids, with known antiviral efficacy, were selected to determine their interactions at five proteins that are known to play a role in the infectivity of SARS-CoV-2. Our results indicated that tribuloside formed significant interactions with the SARS-CoV-2 proteins, Mpro and Nsp12. In contrast, our results suggested that legalon could be a potential inhibitor of ACE2 spike RBD binding site. Compared to all of the compounds, isosilybin had the highest interaction with the Spike-RBD protein. The interaction of all of the compounds with the active site of Nsp15 was significantly weaker than that of tipiracil, which has been reported to have a low to moderate inhibitory efficacy for Nsp15. It is possible that further investigation of the effects of these compounds for the protein targets could help elucidate their exact mechanism of binding. Finally, our results could prove useful for exploring and developing novel natural compounds that have *anti*-SARS-CoV-2 efficacy.

Availability of data and material

During this project, all data is stored on the local backed-up storage servers utilizing the Biocentre Finland storage facility (RB's laboratory is the provider of that service). In addition, after the project was completed, all data were archived and made available through the IDA research data storage service (produced by CSC, the IT Center for Science Ltd, Finland, http://www.csc.fi), so that when needed these data can be retrieved for usage and sharing.

Author's contributions

All authors contributed equally to writing the paper and approved the final manuscript.

Funding

R.B. gratefully acknowledges the financial support of the Academy of Finland (mobility grant) and the Joe, Pentti and Tor Borg Memorial Fund.

Declaration of competing interest

The authors declare that they have no known competing financial interests or personal relationships that could have appeared to influence the work reported in this paper.

Acknowledgement

The Sigrid Jusélius Foundation, Biocenter Finland Bioinformatics and Drug Discovery and Chemical Biology networks, CSC IT Center for Science. Joe, Pentti and Tor Borg Memorial Fund and Prof. Mark Johnson and Dr. Jukka Lehtonen are gratefully acknowledged for the excellent computational infrastructure at the Åbo Akademi University. We would also like to thank Dr. Outi M. H. Salo-Ahen for constructive feedback on the computational part.

Appendix A. Supplementary data

Supplementary data to this article can be found online at https://doi.org/10.1016/j.compbiomed.2021.104464.

References

[1] H. Amawi, G.a.I. Abu Deiab, A.A. A Aljabali, K. Dua, M.M. Tambuwala, COVID-19 pandemic: an overview of epidemiology, pathogenesis, diagnostics and potential vaccines and therapeutics, Ther. Deliv. 11 (2020) 245–268.
[2] P. Pandey, J.S. Rane, A. Chatterjee, A. Kumar, R. Khan, A. Prakash, S. Ray, Targeting SARS-CoV-2 spike protein of COVID-19 with naturally occurring phytochemicals: an in silico study for drug development, J. Biomol. Struct. Dyn. (2020) 1–11.
[3] V.K. Bhardwaj, R. Singh, P. Das, R. Purohit, Evaluation of acridinedione analogs as potential SARS-CoV-2 main protease inhibitors and their comparison with repurposed anti-viral drugs, Comput. Biol. Med. 128 (2021), 104117.
[4] X. Xue, H. Yu, H. Yang, F. Xue, Z. Wu, W. Shen, J. Li, Z. Zhou, Y. Ding, Q. Zhao, Structures of two coronavirus main proteases: implications for substrate binding and antiviral drug design, J. Virol. 82 (2008) 2515–2527.
[5] A. Tariq, R. Mateen, S. Sohail Afzal, M. Saleem, Paromomycin: A Potential Dual Targeted Drug Effectively Inhibits Both Spike (S1) and Main Protease of COVID-19, 2020. Available at SSRN 3575839.
[6] K.K. Chan, D. Dorosky, P. Sharma, S.A. Abbasi, J.M. Dye, D.M. Kranz, A.S. Herbert, E. Procko, Engineering human ACE2 to optimize binding to the spike protein of SARS coronavirus 2, Science 369 (2020) 1261–1265.
[7] A.A. Elfiky, Ribavirin, remdesivir, sofosbuvir, galidesivir, and tenofovir against SARS-CoV-2 RNA dependent RNA polymerase (RdRp): a molecular docking study, Life Sci. 253 (2020), 117592.
[8] X. Deng, M. Hackbart, R.C. Mettelman, A. O'Brien, A.M. Mielech, G. Yi, C.C. Kao, S. C. Baker, Coronavirus nonstructural protein 15 mediates evasion of dsRNA sensors and limits apoptosis in macrophages, Proc. Natl. Acad. Sci. Unit. States Am. 114 (2017) E4251–E4260.
[9] T. Mohammad, A. Shamsi, S. Anwar, M. Umair, A. Hussain, M.T. Rehman, M. F. AlAjmi, A. Islam, M.I. Hassan, Identification of high-affinity inhibitors of SARS-CoV-2 main protease: towards the development of effective COVID-19 therapy, Virus Res. 288 (2020), 198102-198102.
[10] W. Dai, B. Zhang, X.-M. Jiang, H. Su, J. Li, Y. Zhao, X. Xie, Z. Jin, J. Peng, F. Liu, C. Li, Y. Li, F. Bai, H. Wang, X. Cheng, X. Cen, S. Hu, X. Yang, J. Wang, X. Liu, G. Xiao, H. Jiang, Z. Rao, L.-K. Zhang, Y. Xu, H. Yang, H. Liu, Structure-based design of antiviral drug candidates targeting the SARS-CoV-2 main protease, Science (New York, N.Y.) 368 (2020) 1331–1335.
[11] H. Yang, W. Xie, X. Xue, K. Yang, J. Ma, W. Liang, Q. Zhao, Z. Zhou, D. Pei, J. Ziebuhr, Design of wide-spectrum inhibitors targeting coronavirus main proteases, PLoS Biol. 3 (2005), e324.
[12] K. Dubey, R. Dubey, Computation screening of narcissoside a glycosyloxyflavone for potential novel coronavirus 2019 (COVID-19) inhibitor, Biomed. J. 43 (4) (2020) 363–367.
[13] P. Das, R. Majumder, M. Mandal, P. Basak, In-Silico approach for identification of effective and stable inhibitors for COVID-19 main protease (Mpro) from flavonoid based phytochemical constituents of Calendula officinalis, J. Biomol. Struct. Dyn. (2020) 1–16.
[14] D.C. Hall Jr., H.-F. Ji, A search for medications to treat COVID-19 via in silico molecular docking models of the SARS-CoV-2 spike glycoprotein and 3CL protease, Trav. Med. Infect. Dis. (2020), 101646.
[15] N. Vankadari, Arbidol: a potential antiviral drug for the treatment of SARS-CoV-2 by blocking the trimerization of viral spike glycoprotein? Int. J. Antimicrob. Agents (2020), 105998.
[16] J. Shang, Y. Wan, C. Liu, B. Yount, K. Gully, Y. Yang, A. Auerbach, G. Peng, R. Baric, F. Li, Structure of mouse coronavirus spike protein complexed with receptor reveals mechanism for viral entry, PLoS Pathog. 16 (2020), e1008392.
[17] W. Li, M.J. Moore, N. Vasilieva, J. Sui, S.K. Wong, M.A. Berne, M. Somasundaran, J.L. Sullivan, K. Luzuriaga, T.C. Greenough, Angiotensin-converting enzyme 2 is a functional receptor for the SARS coronavirus, Nature 426 (2003) 450–454.
[18] M. Hussain, N. Jabeen, F. Raza, S. Shabbir, A.A. Baig, A. Amanullah, B. Aziz, Structural variations in human ACE2 may influence its binding with SARS-CoV-2 spike protein, J. Med. Virol. 92 (9) (2020) 1580–1586.
[19] F. Li, W. Li, M. Farzan, S.C. Harrison, Structure of SARS coronavirus spike receptor-binding domain complexed with receptor, Science 309 (2005) 1864–1868.
[20] J. Lan, J. Ge, J. Yu, S. Shan, H. Zhou, S. Fan, Q. Zhang, X. Shi, Q. Wang, L. Zhang, Structure of the SARS-CoV-2 spike receptor-binding domain bound to the ACE2 receptor, Nature 581 (2020) 215–220.
[21] A.A. Elfiky, SARS-CoV-2 RNA dependent RNA polymerase (RdRp) targeting: an in silico perspective, J. Biomol. Struct. Dyn. (2020) 1–9.
[22] S. Choudhury, D. Moulick, P. Saikia, M.K. Mazumder, Evaluating the potential of different inhibitors on RNA-dependent RNA polymerase of severe acute respiratory syndrome coronavirus 2: a molecular modeling approach, Med. J. Armed Forces India (2020). In press.
[23] Y. Furuta, T. Komeno, T. Nakamura, Favipiravir (T-705), a broad spectrum inhibitor of viral RNA polymerase, Proc. Jpn. Acad. Ser. B Phys. Biol. Sci. 93 (2017) 449–463.
[24] E. Konkolova, M. Dejmek, H. Hřebabecký, M. Šála, J. Böserle, R. Nencka, E. Boura, Remdesivir triphosphate can efficiently inhibit the RNA-dependent RNA polymerase from various flaviviruses, Antivir. Res. 182 (2020), 104899, 104899.
[25] M. Hackbart, X. Deng, S.C. Baker, Coronavirus endoribonuclease targets viral polyuridine sequences to evade activating host sensors, Proc. Natl. Acad. Sci. Unit. States Am. 117 (2020) 8094–8103.
[26] K. Bhardwaj, L. Guarino, C.C. Kao, The severe acute respiratory syndrome coronavirus Nsp15 protein is an endoribonuclease that prefers manganese as a cofactor, J. Virol. 78 (2004) 12218–12224.
[27] J. Johari, A. Kianmehr, M.R. Mustafa, S. Abubakar, K. Zandi, Antiviral activity of baicalein and quercetin against the Japanese encephalitis virus, Int. J. Mol. Sci. 13 (2012) 16785–16795.
[28] K. Zandi, B.-T. Teoh, S.-S. Sam, P.-F. Wong, M.R. Mustafa, S. AbuBakar, Antiviral activity of four types of bioflavonoid against dengue virus type-2, Virol. J. 8 (2011) 560.
[29] M. Amoros, C. Simões, L. Girre, F. Sauvager, M. Cormier, Synergistic effect of flavones and flavonols against herpes simplex virus type 1 in cell culture. Comparison with the antiviral activity of propolis, J. Nat. Prod. 55 (1992) 1732–1740.
[30] X. Qiu, A. Kroeker, S. He, R. Kozak, J. Audet, M. Mbikay, M. Chrétien, Prophylactic efficacy of quercetin 3-β-Od-glucoside against Ebola virus infection, Antimicrob. Agents Chemother. 60 (2016) 5182–5188.
[31] V.K. Bhardwaj, R. Singh, J. Sharma, V. Rajendran, R. Purohit, S. Kumar, Identification of bioactive molecules from tea plant as SARS-CoV-2 main protease inhibitors, J. Biomol. Struct. Dyn. (2020) 1–10.
[32] J. Sharma, V. Kumar Bhardwaj, R. Singh, V. Rajendran, R. Purohit, S. Kumar, An in-silico evaluation of different bioactive molecules of tea for their inhibition potency against non structural protein-15 of SARS-CoV-2, Food Chem. 346 (2021), 128933.
[33] H. Amawi, C.R. Ashby, A.K. Tiwari, Cancer chemoprevention through dietary flavonoids: what's limiting? Chin. J. Canc. 36 (2017) 1–13.
[34] L.I. da Silva Hage-Melim, L.B. Federico, N.K.S. de Oliveira, V.C.C. Francisco, L. C. Correa, H.B. de Lima, S.Q. Gomes, M.P. Barcelos, I.A.G. Francischini, Virtual screening, ADME/Tox predictions and the drug repurposing concept for future use of old drugs against the COVID-19, Life Sci. (2020), 117963.
[35] J. Zhang, Y. Shan, X. Pan, C. Wang, W. Xu, L. He, Molecular docking, 3D-QSAR Studies, and in silico ADME prediction of p-aminosalicylic acid derivatives as neuraminidase inhibitors, Chem. Biol. Drug Des. 78 (2011) 709–717.

[36] V. Kumar Bhardwaj, R. Purohit, S. Kumar, Himalayan bioactive molecules as potential entry inhibitors for the human immunodeficiency virus, Food Chem. 347 (2021), 128932.
[37] I. Aier, P.K. Varadwaj, U. Raj, Structural insights into conformational stability of both wild-type and mutant EZH2 receptor, Sci. Rep. 6 (2016), 34984.
[38] G. Yadav, R. Rao, U. Raj, P.K. Varadwaj, Computational modeling and analysis of prominent T-cell epitopes for assisting in designing vaccine of ZIKA virus, J. Appl. Pharmaceut. Sci. 7 (2017) 116–122.
[39] H. Kumar, U. Raj, S. Srivastava, S. Gupta, P.K. Varadwaj, Identification of dual natural inhibitors for chronic myeloid leukemia by virtual screening, molecular dynamics simulation and ADMET analysis, Interdiscipl. Sci. Comput. Life Sci. 8 (2016) 241–252.
[40] A. Kumar, V. Mehta, U. Raj, P.K. Varadwaj, M. Udayabanu, R.M. Yennamalli, T. R. Singh, Computational and in-vitro validation of natural molecules as potential acetylcholinesterase inhibitors and neuroprotective agents, Curr. Alzheimer Res. 16 (2019) 116–127.
[41] S. Mahanta, P. Chowdhury, N. Gogoi, N. Goswami, D. Borah, R. Kumar, D. Chetia, P. Borah, A.K. Buragohain, B. Gogoi, Potential anti-viral activity of approved repurposed drug against main protease of SARS-CoV-2: an in silico based approach, J. Biomol. Struct. Dynam. (2020) 1–10.
[42] K. Kant, U.R. Lal, A. Kumar, M. Ghosh, A merged molecular docking, ADME-T and dynamics approaches towards the genus of Arisaema as herpes simplex virus type 1 and type 2 inhibitors, Comput. Biol. Chem. 78 (2019) 217–226.
[43] X. Zhang, S.E. Wong, F.C. Lightstone, Toward Fully Automated High Performance Computing Drug Discovery: a Massively Parallel Virtual Screening Pipeline for Docking and Molecular Mechanics/generalized Born Surface Area Rescoring to Improve Enrichment, ACS Publications, 2014.
[44] S.F. Giardina, D.S. Werner, M. Pingle, P.B. Feinberg, K.W. Foreman, D. E. Bergstrom, L.D. Arnold, F. Barany, Novel, self-assembling dimeric inhibitors of human β tryptase, J. Med. Chem. 63 (2020) 3004–3027.
[45] K. Roos, C. Wu, W. Damm, M. Reboul, J.M. Stevenson, C. Lu, M.K. Dahlgren, S. Mondal, W. Chen, L. Wang, R. Abel, R.A. Friesner, E.D. Harder, OPLS3e: extending Force Field Coverage for Drug-Like Small Molecules, J. Chem. Theor. Comput. 15 (2019) 1863–1874.
[46] J.R. Greenwood, D. Calkins, A.P. Sullivan, J.C. Shelley, Towards the comprehensive, rapid, and accurate prediction of the favorable tautomeric states of drug-like molecules in aqueous solution, J. Comput. Aided Mol. Des. 24 (2010) 591–604.
[47] J.C. Shelley, A. Cholleti, L.L. Frye, J.R. Greenwood, M.R. Timlin, M. Uchimaya, Epik: a software program for pK(a) prediction and protonation state generation for drug-like molecules, J. Comput. Aided Mol. Des. 21 (2007) 681–691.
[48] H.M. Berman, J. Westbrook, Z. Feng, G. Gilliland, T.N. Bhat, H. Weissig, I. N. Shindyalov, P.E. Bourne, The protein data bank, Nucleic Acids Res. 28 (2000) 235–242.
[49] Z. Jin, X. Du, Y. Xu, Y. Deng, M. Liu, Y. Zhao, B. Zhang, X. Li, L. Zhang, C. Peng, Y. Duan, J. Yu, L. Wang, K. Yang, F. Liu, R. Jiang, X. Yang, T. You, X. Liu, X. Yang, F. Bai, H. Liu, X. Liu, L.W. Guddat, W. Xu, G. Xiao, C. Qin, Z. Shi, H. Jiang, Z. Rao, H. Yang, Structure of Mpro from SARS-CoV-2 and discovery of its inhibitors, Nature 582 (2020) 289–293.
[50] M.A. Alamri, M. Tahir Ul Qamar, M.U. Mirza, R. Bhadane, S.M. Alqahtani, I. Muneer, M. Froeyen, O.M.H. Salo-Ahen, Pharmacoinformatics and molecular dynamics simulation studies reveal potential covalent and FDA-approved inhibitors of SARS-CoV-2 main protease 3CL(pro), J. Biomol. Struct. Dynam. (2020) 1–13.
[51] R.A. Friesner, R.B. Murphy, M.P. Repasky, L.L. Frye, J.R. Greenwood, T.A. Halgren, P.C. Sanschagrin, D.T. Mainz, Extra precision Glide: docking and scoring incorporating a model of hydrophobic enclosure for Protein−Ligand complexes, J. Med. Chem. 49 (2006) 6177–6196.
[52] T.A. Halgren, R.B. Murphy, R.A. Friesner, H.S. Beard, L.L. Frye, W.T. Pollard, J. L. Banks, Glide: a new approach for rapid, accurate docking and scoring. 2. Enrichment factors in database screening, J. Med. Chem. 47 (2004) 1750–1759.
[53] R.A. Friesner, J.L. Banks, R.B. Murphy, T.A. Halgren, J.J. Klicic, D.T. Mainz, M. P. Repasky, E.H. Knoll, M. Shelley, J.K. Perry, D.E. Shaw, P. Francis, P.S. Shenkin, Glide: a new approach for rapid, accurate docking and scoring. 1. Method and assessment of docking accuracy, J. Med. Chem. 47 (2004) 1739–1749.
[54] M.P. Jacobson, D.L. Pincus, C.S. Rapp, T.J. Day, B. Honig, D.E. Shaw, R.A. Friesner, A hierarchical approach to all-atom protein loop prediction, Proteins 55 (2004) 351–367.
[55] M.P. Jacobson, R.A. Friesner, Z. Xiang, B. Honig, On the role of the crystal environment in determining protein side-chain conformations, J. Mol. Biol. 320 (2002) 597–608.
[56] K.J. Bowers, E. Chow, H. Xu, R.O. Dror, M.P. Eastwood, B.A. Gregersen, J. L. Klepeis, I. Kolossvary, M.A. Moraes, F.D. Sacerdoti, J.K. Salmon, Y. Shan, D. E. Shaw, Scalable algorithms for molecular dynamics simulations on commodity clusters, in: Proceedings of the 2006 ACM/IEEE Conference on Supercomputing, Association for Computing Machinery, Tampa, Florida, 2006, p. 84, es.
[57] H.J. Berendsen, J.P. Postma, W.F. van Gunsteren, J. Hermans, INteraction Models for Water in Relation to Protein Hydration, Intermolecular Forces, Springer1981, pp. 331-342.
[58] S. Nosé, A unified formulation of the constant temperature molecular dynamics methods, J. Chem. Phys. 81 (1984) 511–519.
[59] S. Nosé, A molecular dynamics method for simulations in the canonical ensemble, Mol. Phys. 52 (1984) 255–268.
[60] W.G. Hoover, Canonical dynamics: equilibrium phase-space distributions, Phys. Rev. 31 (1985) 1695–1697.
[61] G.J. Martyna, D.J. Tobias, M.L. Klein, Constant pressure molecular dynamics algorithms, J. Chem. Phys. 101 (1994) 4177–4189.
[62] C. Predescu, A.K. Lerer, R.A. Lippert, B. Towles, J.P. Grossman, R.M. Dirks, D. E. Shaw, The u-series: a separable decomposition for electrostatics computation with improved accuracy, J. Chem. Phys. 152 (2020), 084113.
[63] A. Hasan, B.A. Paray, A. Hussain, F.A. Qadir, F. Attar, F.M. Aziz, M. Sharifi, H. Derakhshankhah, B. Rasti, M. Mehrabi, A review on the cleavage priming of the spike protein on coronavirus by angiotensin-converting enzyme-2 and furin, J. Biomol. Struct. Dyn. (2020) 1–9.
[64] A.R. Bourgonje, A.E. Abdulle, W. Timens, J.-L. Hillebrands, G.J. Navis, S.J. Gordijn, M.C. Bolling, G. Dijkstra, A.A. Voors, A.D. Osterhaus, P.H. van der Voort, D. J. Mulder, H. van Goor, Angiotensin-converting enzyme 2 (ACE2), SARS-CoV-2 and the pathophysiology of coronavirus disease 2019 (COVID-19), J. Pathol. 251 (2020) 228–248.
[65] J. Ahmad, S. Ikram, F. Ahmad, I.U. Rehman, M. Mushtaq, SARS-CoV-2 RNA Dependent RNA polymerase (RdRp) – a drug repurposing study, Heliyon 6 (2020), e04502.
[66] S. Vardhan, S.K. Sahoo, In silico ADMET and molecular docking study on searching potential inhibitors from limonoids and triterpenoids for COVID-19, Comput. Biol. Med. 124 (2020), 103936-103936.
[67] F.M.A. da Silva, K.P.A. da Silva, L.P.M. de Oliveira, E.V. Costa, H.H. Koolen, M.L. B. Pinheiro, A.Q.L. de Souza, A.D.L. de Souza, Flavonoid glycosides and their putative human metabolites as potential inhibitors of the SARS-CoV-2 main protease (Mpro) and RNA-dependent RNA polymerase (RdRp), Mem. Inst. Oswaldo Cruz (2020) 115.
[68] S.T. Ngo, H.M. Nguyen, L.T. Thuy Huong, P.M. Quan, V.K. Truong, N.T. Tung, V. V. Vu, Assessing potential inhibitors of SARS-CoV-2 main protease from available drugs using free energy perturbation simulations, RSC Adv. 10 (2020) 40284–40290.
[69] W. Li, M.J. Moore, N. Vasilieva, J. Sui, S.K. Wong, M.A. Berne, M. Somasundaran, J.L. Sullivan, K. Luzuriaga, T.C. Greenough, H. Choe, M. Farzan, Angiotensin-converting enzyme 2 is a functional receptor for the SARS coronavirus, Nature 426 (2003) 450–454.
[70] T.Z. Kristiansen, J. Bunkenborg, M. Gronborg, H. Molina, P.J. Thuluvath, P. Argani, M.G. Goggins, A. Maitra, A. Pandey, A proteomic analysis of human bile, Mol. Cell. Proteomics : MCP 3 (2004) 715–728.
[71] R. Chen, X. Jiang, D. Sun, G. Han, F. Wang, M. Ye, L. Wang, H. Zou, Glycoproteomics analysis of human liver tissue by combination of multiple enzyme digestion and hydrazide chemistry, J. Proteome Res. 8 (2009) 651–661.
[72] P. Towler, B. Staker, S.G. Prasad, S. Menon, J. Tang, T. Parsons, D. Ryan, M. Fisher, D. Williams, N.A. Dales, M.A. Patane, M.W. Pantoliano, ACE2 X-ray structures reveal a large hinge-bending motion important for inhibitor binding and catalysis, J. Biol. Chem. 279 (2004) 17996–18007.
[73] M. Romano, A. Ruggiero, F. Squeglia, G. Maga, R. Berisio, A structural view of SARS-CoV-2 RNA replication machinery: RNA synthesis, proofreading and final capping, Cells 9 (2020) 1267.
[74] B.G. Vijayakumar, D. Ramesh, A. Joji, T. Kannan, In silico pharmacokinetic and molecular docking studies of natural flavonoids and synthetic indole chalcones against essential proteins of SARS-CoV-2, Eur. J. Pharmacol. 886 (2020), 173448.